diborides. Lattice parameters and interatomic distances of this series are listed in Table 1. A notable feature of the series is the unusually large metal–boron separation in both $PuB_2$ and $UB_2$. For the transition-metal diborides the experimental metal–boron distance exceeds the 'contact' distance (i.e. the sum of the close packed radii) by only 0·06–0·08 Å, whereas in $UB_2$ and $PuB_2$, the measured metal–boron distances exceed the calculated distances by 0·34, and 0·21 Å respectively.

A tetraboride phase was formed at 1200 °C. when the atomic percentage of boron was greater than 70. The proportion of this phase formed increased rapidly with boron content up to 85 at.% boron, but thereafter decreased with increasing boron content. The $PuB_4$ phase is isomorphous with $UB_4$ and is tetragonal, with $a = 7{\cdot}10$ and $c = 4{\cdot}014$ Å. The structure of $UB_4$ is given by Zalkin & Templeton (1950) who showed the space group to be *P*4/*mbm* and the atomic positions:

Metal in ±(0·31, 0·81, 0; 0·21, 0·31, 0).
4 B I in ±(0, 0, 0·2; 0·5, 0·5, 0·2).
4 B II ±(0·1, 0·6, 0·5; 0·4, 0·1, 0·5).
8 B III in ±(0·2, 0·04, 0·5; 0·7, 0·46, 0·5; 0·04, 0·2, 0·5; 0·54, 0·7, 0·5).

Using the lattice parameters found for plutonium tetraboride, the metal-boron distances are Pu–B I 2·77, Pu–B II 2·84, Pu–B III 2·47 Å i.e. the plutonium and the B III boron atoms are in contact.

Plutonium hexaboride was also formed at 1200 °C. when the amount of boron present exceeded 70 at.%. The proportion of the hexaboride formed increased steadily with increasing boron content. The structure is simple-cubic $CaB_6$-type and is isomorphous with $ThB_6$. With metal atoms at (0, 0, 0) and boron atoms at $\pm[(\frac{1}{2}, \frac{1}{2}, 0{\cdot}21), (\frac{1}{2}, 0{\cdot}21, \frac{1}{2}), (0{\cdot}21, \frac{1}{2}, \frac{1}{2})]$ the plutonium–boron distance is 2·92 Å, whereas the 'contact' distance is 2·47 Å. The boron atoms are in close contact since the boron–boron distance is 1·75 Å. The lattice parameter varies from 4·115 ± 0·001 to 4·140 ± 0·001 Å, suggesting that the hexaboride phase is not stoichiometric, and that excess boron is present in the structure.

We should like to thank Mrs G. Tyson for her help with this work and the Managing Director, Production Group, U.K.A.E.A. for permission to publish this paper.

## References

POST, B., GLASER, F. W. & MOSKOWITZ, D. (1954). *Acta Met.* **2**, 20.

ZALKIN, A. & TEMPLETON, D. H. (1950). *J. Chem. Phys.* **18**, 391.

---

*Acta Cryst.* (1960). **13**, 448

# Heat treatment of evaporated carbon films.

By J. KAKINOKI, K. KATADA, and T. HANAWA, *The Institute of Polytechnics. Osaka City University, Minami-ogi-machi, Kita-ku, Osaka, Japan*

(*Received* 12 *January* 1960)

The structure analysis of evaporated carbon films deposited at room temperature was reported in the previous paper (Kakinoki *et al.*, 1960). In this note, we will report the structural change of these films when subjected to heat treatment.

Carbon films deposited at room temperature are attached on specimen holders made of thin carbon plates and heated to desired temperatures in a vacuum furnace. The film temperature is estimated by a small thermocouple placed near the specimen. The specimens used are taken from the same lot deposited at the same time, and they have a thickness of 240 Å. The highest temperatures attained in each treatment are 500, 700, 800, 900, 1000, and 1200 °C., respectively. The rate of temperature raise is about 100 °C. per min. Each specimen is kept at the highest temperature for 1 min., and then allowed to cool to room temperature, the rate of temperature decrease being very rapid.

Electron-diffraction diagrams show gradual change in the structure with increase of the temperature in heat treatment. These behaviours are shown in Figs. 1 and 2. Photographs in Fig. 1 are taken with $s^2$-sector under normal incidence, their intensity curves being represented in Fig. 2. At about 1200 °C., the diffraction pattern changes into sharp Debye–Scherrer rings with asymmetric line profiles, and they are all indexed with (*hk*0) of graphite having a lattice constant of $a = 2{\cdot}456$ Å, their spacings being listed in Table 1. No (*hkl*) ($l \neq 0$)

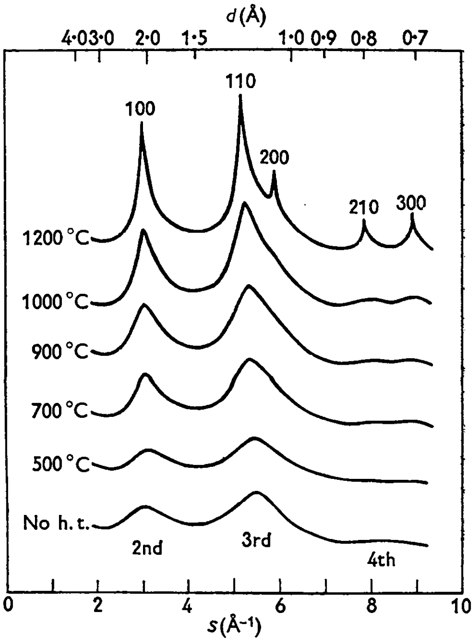

Fig. 2. Intensity curves of the photographs in Fig. 1 ($s = 2\pi/d = 4\pi \sin\theta/\lambda$).

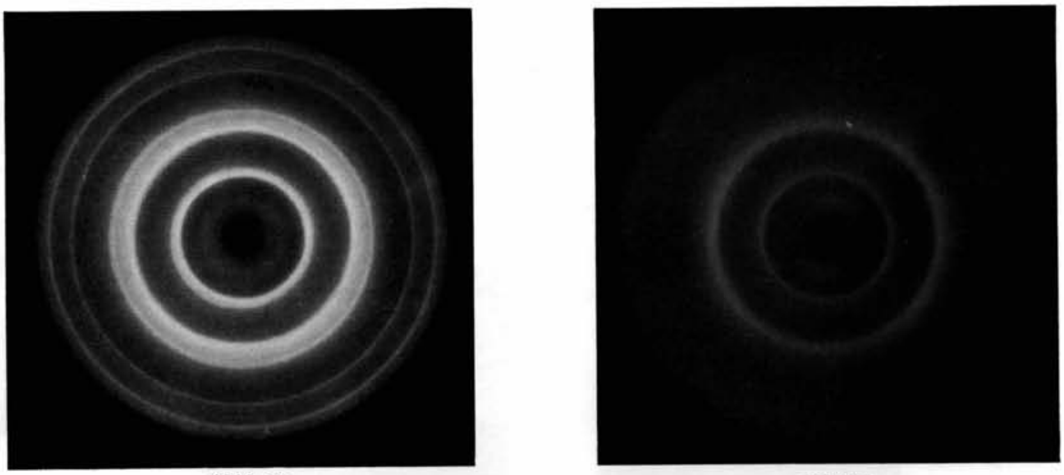

1200 °C 1000 °C

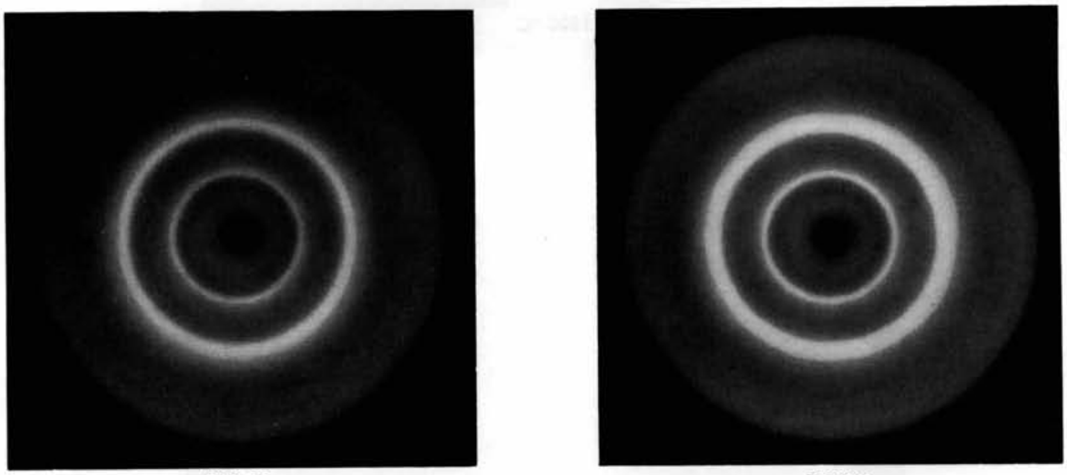

900 °C 700 °C

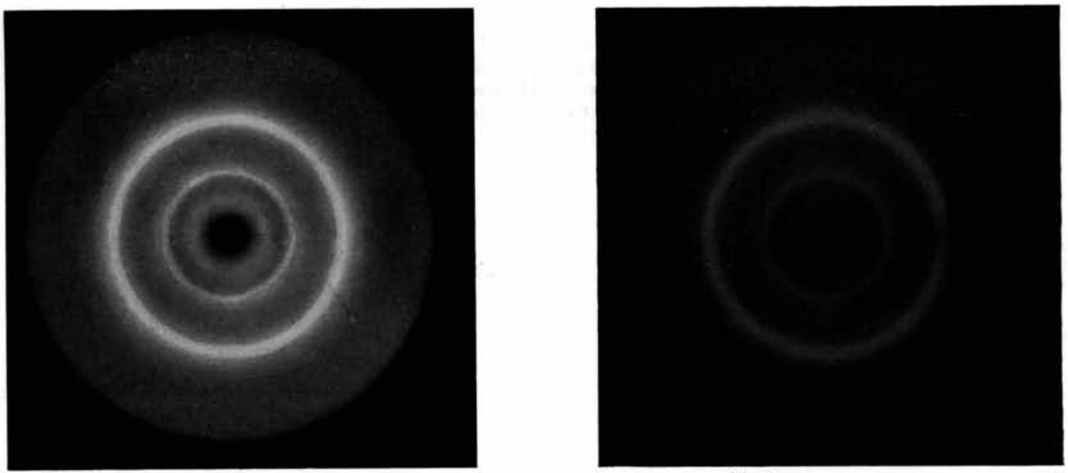

500 °C No heat treatment

Fig. 1. Electron-diffraction photographs of evaporated carbon films heated at various temperatures, taken with $s^2$-sector under normal incidence. (Extraneous rings due to slight cracks on the sector can be seen inside of the (100) line.)

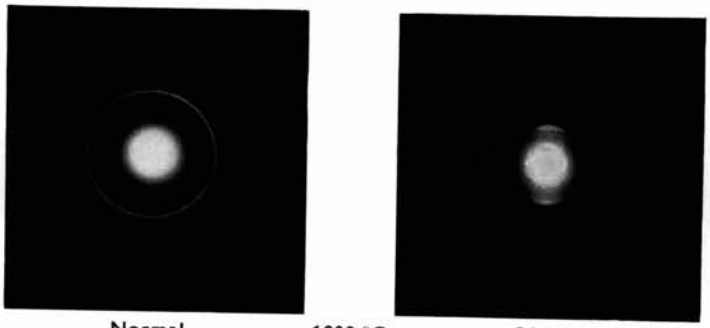

Normal 1200 °C Oblique

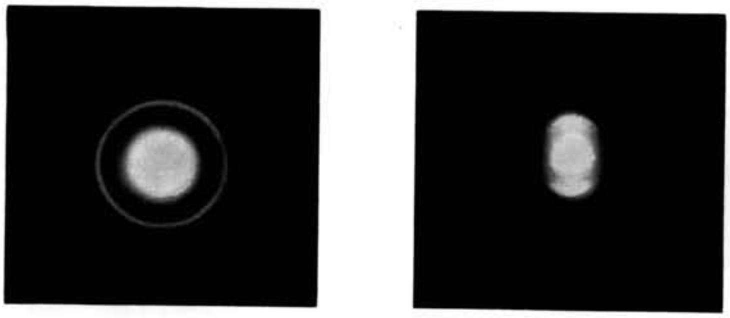

Normal 900 °C Oblique

Fig. 3. Electron-diffraction photographs of evaporated carbon films heated at 900 and 1200 °C., taken without sector under normal and oblique incidences, respectively. In the latter case, the specimen film is rotated 45° about an axis normal to the incident beam. The horizontal line through the center of the photograph corresponds to the projection of the axis.

Table 1. *Spacings of* (*hkl*) *lines of evaporated carbon film heated at* 1200 °C.

Values of $d_c$ are calculated from graphite lattice having $a = 2{\cdot}456$ Å. For comparison, positions of halos on diffraction pattern of carbon film without being heat-treated are also listed

$(s = 2\pi/d = 4\pi \sin\,\theta/\lambda)$

| | Carbon film heated at 1200 °C. | | | | Carbon film without being heat-treated |
|---|---|---|---|---|---|
| *hkl* | $d_c$ (Å) | $d_o$ (Å) | $s_o$ (Å$^{-1}$) | No. | $s_o$ (Å$^{-1}$) |
| (002) | | 3·408 | 1·84 | 1 | 1·2 |
| 100 | 2·127 | 2·120 | 2·96 | 2 | 2·9 |
| (004) | | 1·71 | 3·67 | | |
| 110 | 1·228 | 1·228 | 5·12 | 3 | 5·5 |
| 200 | 1·063 | 1·063 | 5·91 | | |
| 210 | 0·804 | 0·8045 | 7·81 | | |
| 300 | 0·709 | 0·7089 | 8·86 | 4 | 8·6 |
| 220 | 0·614 | 0·6135 | 10·2 | 5 | 10·4 |
| 310 | 0·590 | 0·5905 | 10·6 | | |
| 400 | 0·532 | 0·532 | 11·8 | | |
| 320 | 0·488 | 0·487 | 12·9 | | |
| 410 | 0·464 | 0·4641 | 13·5 | 6 | 13·5 |
| 500 | 0·425 | | | | |
| 330 | 0·409 | 0·409 | 15·4 | | |
| 420 | 0·402 | 0·403 | 15·6 | | |
| 510 | 0·382 | 0·381 | 16·5 | | |
| 600 | 0·354 | 0·353 | 17·8 | | |
| 430 | 0·350 | | | | |
| 520 | 0·341 | 0·341 | 18·4 | 7 | 18·1 |
| 610 | 0·324 | | | | |
| 440 | 0·307 | 0·305 | 20·6 | | |
| 530, 700 | 0·304 | | | | |
| 620 | 0·295 | | | | |
| 710 | 0·282 | 0·281 | 22·4 | 8 | 22·4 |
| 540 | 0·272 | | | | |
| 630 | 0·268 | 0·267 | 23·5 | | |
| 800 | 0·266 | | | | |
| | | | | 9 | 24·8 |
| | | | | 10 | 28·5 |
| | | | | 11 | 32 |

lines can be observed. When the incident beam is normal to the surface of the film, the basal reflections (002) and (004) do not appear, but when the beam is inclined to the surface, they do appear as arcs which run across the vertical line as shown in Fig. 3. The interlayer spacing is estimated to be 3·41 Å. From these observations, it is obvious that films heated at higher temperatures have the random layer structure, each layer having orientation parallel to the film surface.

It is remarkable to note that the three-dimensional random network structure (composed of graphite-like and diamond-like configurations) of evaporated carbon film transforms into the random layer structure with prefered orientation at elevated temperature. The random layer structure is frequently found in the so-called 'amorphous' carbons, which are generally prepared by any heat treatment of about 1000 °C. and are known to transform into crystalline graphite at the higher temperature (1000 ∼ 3000 °C.) with some exceptional cases (Franklin, 1951). The temperatures in the present treatment are comparable with those in preparation of other 'amorphous' carbons, and it is a future problem whether the obtained random layer structure will change to graphite crystal structure by further heat treatment or not. Extended study is now proceeding, and detailed analysis will be reported later.

## References

Franklin, R. E. (1951). *Proc. Roy. Soc. Lond.* A, **209**, 196.

Kakinoki, J., Katada, K., Hanawa, T. & Ino, T. (1960). *Acta Cryst.* **13**, 171.

---

*Acta Cryst.* (1960). **13**, 449

## Comparison of three structure determinations for germanium selenide, GeSe.*

By C. R. Kannewurf, A. Kelly,† and R. J. Cashman, *Technological Institute, Northwestern University, Evanston, Illinois, U.S.A.*

(*Received* 22 *December* 1959)

The recent success at this laboratory in the preparation of high purity single crystals of germanium sulfide, GeS, and the subsequent optical and electrical measurements with these crystals prompted the continuation of similar measurements with other $IV_b$–$VI_b$ compounds from these groups in the periodic table, especially those of germanium (Betz, 1958). It was found that germanium selenide, GeSe, could be prepared in a manner similar to that for GeS. A detailed description of the methods and techniques involved in producing high purity single crystals of GeS and GeSe is now in preparation and will be submitted soon for publication elsewhere.

At the beginning of this investigation only one previous publication by Ivanov-Emin (1940) had reported any work with solid GeSe. Preparation of the material, a few chemical properties, and a tentative crystal system assignment were given. Preliminary X-ray data obtained here were in disagreement with this Russian work, and therefore a complete structure analysis of GeSe was started in early 1958. When the present work was nearly completed a detailed structure analysis was reported by Okazaki (1958). Our results are in good agreement with those of Okazaki.

In Table 1, the complete disagreement with the Russian work is quite evident. In that determination, the crystal system and lattice parameters were deduced from only 18 powder photograph lines. The *d* values and intensities of these lines, with the possible exception of three or four, do not show any recognizable correspond-

---

* Supported in part by the Department of the Navy, Bureau of Ships, Washington, D.C.

† Now at the Department of Metallurgy, University of Cambridge, Cambridge, England.